







## STRUCTURAL AND PHASE STATES OF RHODIUM DOPED SILICON MONOCRYSTALS

 Akramjon Y. Boboev<sup>1</sup>,  Sherzod A. Makhmudov<sup>2</sup>,  Avaz K. Rafikov<sup>2</sup>,  Ziyodjon M. Ibrokhimov<sup>3</sup>,  
Rakhmat M. Mansurov<sup>4</sup>,  Nuritdin Y. Yunusaliyev<sup>1</sup>,  Biloliddin M. Ergashev<sup>5</sup>

<sup>1</sup>Andijan State University named after Z.M. Babur, Andijan, Uzbekistan

<sup>2</sup>Institute of Nuclear Physics, Academy of Sciences of the Republic of Uzbekistan

<sup>3</sup>Andijan State Technical Institute, Andijan, Uzbekistan

<sup>4</sup>Academic Lyceum No. 1 of the Ministry of Internal Affairs of the Republic of Uzbekistan

<sup>5</sup>Andijan State Pedagogical Institute, Andijan, Uzbekistan

\*Corresponding Author e-mail: [aboboevscp@gmail.com](mailto:aboboevscp@gmail.com)

Received February 28, 2026; revised April 22, 2026; accepted May 6, 2026

In this paper, the structural and phase states of silicon (Si) monocrystals doped with rhodium (Rh) atoms were investigated. For the study, n-type silicon samples doped with rhodium, grown by the Chokralsky method, were selected. Rhodium atoms were introduced via thermal diffusion at 1300°C, and the samples were cooled under both slow and rapid cooling regimes. The resulting data were evaluated using X-ray diffraction (XRD) analysis. In the control samples, heat treatment resulted in the formation of secondary phases such as SiP<sub>2</sub> and SiO<sub>2</sub>, which were shown to be associated with background impurities, particularly oxygen atoms. In the rhodium-alloyed and slow-cooled sample, the SiRh<sub>3</sub> phase formed, and the crystal lattice remained relatively stable. This indicates that the rhodium atoms have the ability to reduce internal stresses and relax the lattice. In the rapid cooling regime, the RhO<sub>2</sub> oxide phase appeared, and an increase in micro-stresses and crystal defects was observed. The results indicate that rhodium doping is an effective method for controlling the structure, phase composition, and electrical properties of silicon monocrystals. This research is of significant importance for semiconductor materials, microelectronics, and solar cells.

**Keywords:** Silicon; Rhodium; Phosphorus; Diffusion; Impurity; Oxygen; Secondary phases; XRD; Defects; Microstrain

**PACS:** 61.72.U

### INTRODUCTION

At present, one of the key priorities in solid-state physics and semiconductor technology is the atomistic control of materials' electro-physical properties. Single-crystal silicon (Si), owing to its technological versatility and widespread natural abundance, remains the "foundation" of modern micro- and nanoelectronics. However, the reduction of modern devices (high-frequency transistors, power thyristors, and high-efficiency solar cells) to the nanometre scale has drastically increased the demand for structural perfection of the material. Any uncontrolled defect or impurity atom in the crystal lattice serves as a primary factor in reducing the device's useful coefficient of performance. Moreover, oxygen atoms, which give rise to both "beneficial" and "deleterious" states in silicon monocrystals grown by the Czochralski method, are also the most common technological background impurities (with a concentration of up to 10<sup>17</sup>–10<sup>18</sup> cm<sup>3</sup>) [1]. In some cases, oxygen atoms strengthen the crystal lattice and restrict dislocation movement [2]. During heat treatment processes (at around 450 °C and 650 °C), oxygen atoms form 'thermal donors', which unexpectedly alters the material's relative resistance [3]. Furthermore, the uneven distribution of oxygen precipitates (SiO<sub>x</sub>) induces high mechanical stresses within the crystal, leading to the scattering of charge carriers and energy loss [4].

Legating silicon with 4d transition metals, particularly rhodium (Rh), is considered one of the most promising methods for modifying material properties. Rhodium atoms in silicon's forbidden band give rise to deep energy levels (for example, at  $E_c - 0.32$  eV and  $E_v + 0.35$  eV) that exhibit both donor and acceptor characteristics [5]. This allows for the wide range control of the charge carriers' recombination rate. Furthermore, due to the high diffusion coefficient of rhodium in silicon, a uniform distribution of the impurities throughout the monocrystal can be achieved by introducing it via thermal diffusion [6]. Furthermore, rhodium atoms also possess the ability to clean the crystal's active areas by collecting (gettering) oxygen and other technological impurities around them [7]. The formation of Rh-O complexes enhances the semiconductor's resistance to high temperatures [8]. This prevents the material from degrading during the high-temperature thermal oxidation and diffusion stages of the manufacturing process. At the same time, in rhodium-doped silicon, radiation-induced defects (for example, A centres or E centres) interact with the rhodium atoms and lose their electrical activity [9]. In this regard, the investigation of the structural properties and phase states of complexes of silicon with rhodium and oxygen atoms not only allows for an understanding of fundamental processes in solid-state physics, but also allows for the creation of new materials that can operate stably under extreme conditions for practical nanoelectronics. However, despite the great interest in rhodium-doped silicon crystal, research has been mainly limited to studying its electrical and recombination-related properties. The structural changes and phase formation processes that occur in bulk silicon single crystals during rhodium diffusion have not been sufficiently studied. In particular, the

relationship between high-temperature rhodium diffusion, the formation of secondary phases, and the relaxation of internal micro-strains in the silicon lattice has not yet been systematically experimentally determined.

Therefore, in this research work, we aimed to conduct a fundamental analysis of the mechanisms of structural changes and phase formation that occur in bulk silicon single crystals during rhodium diffusion. The scientific novelty of the work lies in the first experimental confirmation that the formation of secondary phases  $\text{SiRh}_3$  and  $\text{RhO}_2$  under high-temperature diffusion and controlled cooling regimes leads to a significant reduction in internal micro-strains in the silicon crystal lattice. Thus, in contrast to previous studies that focused mainly on electrical properties, this work reveals the unique role of rhodium in the structural stabilization of the silicon matrix and provides new insights into the phase formation processes in the Rh-Si-O system.

## MATERIALS AND METHODS

As the research object, n-type monocrystalline silicon samples, phosphorus-doped and grown by the Czochralski method, were selected. For the experiments, the samples were prepared with dimensions of  $10 \times 10 \times 1 \text{ mm}^3$ . To ensure the cleanliness of the sample surfaces, they underwent a two-stage treatment: first the surfaces were mechanically polished, then chemically treated to completely remove organic and inorganic contaminants. The doping process of the silicon samples was carried out in two distinct stages. In the first stage, rhodium (Rh) metal was deposited onto the surface of the silicon substrates using a VUP-4 vacuum system. Subsequently, the samples were placed into high-purity quartz ampoules, which were then evacuated to a residual pressure of  $5\text{--}6 \cdot 10^{-2} \text{ mmHg}$  and hermetically sealed. Thermal diffusion was performed at a constant temperature of  $1300^\circ\text{C}$  for 10 hours. This specific duration was selected to ensure equilibrium and facilitate a uniform distribution of Rh atoms throughout the bulk volume of the samples. Following the diffusion process, the samples were subjected to two different cooling regimes to investigate their structural impact: a) rapid Quenching: Samples were quickly removed from the furnace and immersed in a specialized cooling oil achieving a cooling rate of approximately  $300^\circ\text{C}/\text{min}$ ; b) Slow Cooling: Samples remained inside the furnace, where the temperature was gradually decreased at a controlled rate of  $5\text{--}20^\circ\text{C}/\text{min}$ . These contrasting cooling modes allowed for a comparative analysis of the phase transformations and the relaxation of internal micro-strains within the Rh-Si system.

The structural and phase states of the investigated samples were monitored using an Empyrean Malvern X-ray diffractometer. X-ray diffraction measurements were carried out in Bragg–Brentano geometry, with a continuous scan speed of  $1^\circ/\text{min}$  over a  $2\theta$  range of  $10^\circ$  to  $80^\circ$ . The angular step was set to 0.02 degrees. The graphical analysis and peak integration were performed using Origin software package.

## RESULTS AND DISCUSSION

In the study, the X-ray diffraction state of n-Si<P> samples prepared without deliberately introducing impurity atoms (for example, rhodium) was evaluated (Figure 1, green line).

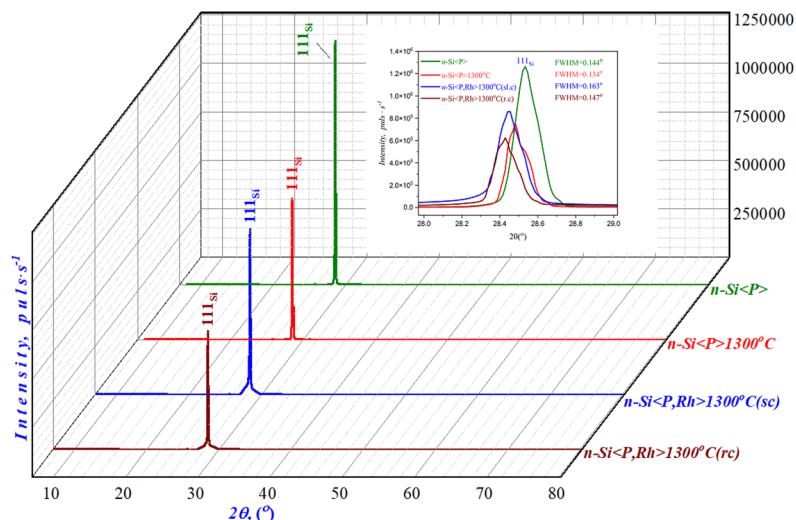


**Figure 1.** XRD patterns of n-Si<P> and Rh-doped n-Si<P,Rh> samples before and after  $1300^\circ\text{C}$  heat treatment under slow-cooling (sc) and rapid-cooling (rc) regimes.

This, in turn, involves identifying the secondary phases that arise from the natural structural changes in the silicon crystal lattice under heat treatment, from background impurities (particularly oxygen) and from the redistribution of phosphorus atoms. In the X-ray diffraction pattern of the control sample, a high-intensity ( $I = 1268300 \text{ imp/s}$ ) diffraction reflection corresponding to the  $(111)_{\text{Si}}$  crystallographic plane was observed at  $2\theta = 28.54^\circ$ . The high intensity and selective nature of this peak indicate that the sample surface is oriented with respect to the  $(111)$  crystallographic direction. Using the interplanar distance  $d = 3.125 \text{ \AA}$  for the  $(111)$  reflection, the lattice constant of the n-Si<P> samples was determined to be  $a \approx 5.4126 \text{ \AA}$ . Furthermore, using the experimental values of this orientation, the size of the constituent sub-crystallites was calculated to be  $D \approx 59.7 \text{ nm}$ . This value indicates that, while the silicon remains monocrystalline, there

are a certain number of boundary regions and microdefects within the volume [10]. At the same time, additional low-intensity peaks were also observed in the X-ray diffraction spectrum of the control sample (see Figures 2a, b and c). In particular, the observation of the (200) reflection of the SiP<sub>2</sub> phase at  $2\theta = 30.90^\circ$  suggests that part of the phosphorus impurity may be locally concentrated in regions prone to chemical bonding with silicon. Using the experimental values of this reflection, recalculations based on these compounds determined that the size of the resulting polycrystallite domains is  $D \approx 75.1$  nm. The observation of the SiP<sub>2</sub> phase is often explained by the redistribution of phosphorus and its binding at certain “energetically favorable” centres during high-temperature treatments [11]. In the control sample, traces of oxide phases formed in the presence of oxygen were also detected. At  $2\theta = 42.43^\circ$ , the (211) reflection corresponding to the SiO<sub>2</sub> phase was observed. The FWHM for this reflection was larger, and the calculated nanocrystallite size was around  $D \approx 25$  nm. Furthermore, for this SiO<sub>2</sub> phase, the lattice constants characteristic of the trigonal P321 space group was determined to be  $a = b \approx 5.031$  Å and  $c \approx 5.527$  Å. The relatively small size of the oxide nanocrystals is explained by the precipitation of oxygen atoms mainly at the grain boundaries, around dislocations, or in near-surface layers.

In the next stage, the X-ray diffraction characteristics of n-Si<P> samples heat-treated at 1300°C for ten hours were studied (Figure 1, red line). Typically, heat treatment leads to a redistribution of internal stresses in the crystal lattice, are used to redistribute internal stresses in the crystal lattice following heat treatment, accelerate diffusion processes, change the configuration of defects, and bring background impurities (oxygen, carbon) and phosphorus atoms to a dynamic equilibrium state [12]. Under such conditions, the structural evolution is assessed by changes in lattice constants, shifts in diffraction peaks at various angles, and variations in intensity and half-width. After heat treatment, the (111)<sub>Si</sub> reflection was observed to shift to  $2\theta = 28.36^\circ$ . The shift of this reflection towards smaller angles indicates a slight change in the interplanar distance ( $d = 3.131$  Å) and an increase in the lattice constant  $a \approx 5.423$  Å. Furthermore, the intensity of the (111)<sub>Si</sub> reflection decreased to  $I = 758700$  imp/s. This, in turn, indicates an increase in microdistortions at the surface, an increase in diffusion centres due to diffusion, and an increase in the proportion of secondary phases in some domains and at boundaries [13]. At the same time, it was determined that the size of the sub-crystals ( $D \approx 64.9$  nm) increased, based on experimental values of the (111)<sub>Si</sub> reflection. It is associated with the ‘coarsening’ of subgrain boundaries resulting from heat treatment, a process that is thermodynamically favorable at elevated temperatures [14]. However, the increase in subgrain size accompanied by a decrease in intensity indicates an uneven structural order in the crystal lattice, i.e., enlargement in some areas and an increase in defects and micro-stresses in others [15]. After heat treatment at 1300°C, the phase corresponds to SiP<sub>2</sub>. The (200) peak was observed at  $2\theta = 30.86^\circ$ , but its intensity had decreased and the calculated polycrystallite domain size was around  $D \approx 62.6$  nm. This suggests that some of the phosphorus undergoes remelting or diffuses into less localized regions [16]. In other words, at elevated temperatures phosphorus atoms tend to distribute relatively uniformly throughout the silicon volume, although it is also possible that a stable phase state is maintained at certain energetically favourable centres [17]. During the growth of silicon monocrystals by the Czochralski method, the incorporation of a certain amount of background impurities such as oxygen and carbon into the crystal volume is well known in practice. Oxygen atoms often form clusters in interstitial sites or as Si–O bonds, and during thermal treatments can evolve into SiO<sub>x</sub> and SiO<sub>2</sub> crystallites. Therefore, the appearance of peaks characteristic of the SiO<sub>2</sub> phase in the X-ray diffraction patterns confirms the active participation of the background impurities.

The formation of SiO<sub>2</sub> nanocrystallites with dimensions of around 20–30 nm acts as a barrier to the movement of charge carriers in the oxide precipitates, creating recombination centers or, conversely, under certain technological conditions, it can increase the bulk purity by collecting harmful impurities through a “gettering” effect. As a qualitative assessment of micro-stresses, the presence of ‘forbidden’ reflections such as (222)<sub>Si</sub>, which are weakly visible in the normally ideal diamond-like structure, and their intensity ratios are used (see red line in Fig. 2c). The amount of formed micro-stresses can be estimated by  $I(222)/I(111)$  can be estimated from the  $I(222)/I(111)$  ratio  $\approx 2.5 \cdot 10^{-3}$  [18]. This value is much larger than the ideal  $\sim 10^{-4}$  order of magnitude, indicating the presence of local deformations, dislocations, boundary regions, and a non-uniform distribution of inclusions in the crystal lattice [18]. During heat treatment, such micro-stresses lead to a reduction in internal stresses through the annihilation and reorganization of defects, as well as the formation of oxygen precipitates, secondary phases (SiP<sub>2</sub>, SiO<sub>2</sub>) and their lattice constant mismatches.

Analysis of the X-ray diffraction patterns of n-Si<P,Rh> samples prepared under slow-cooling conditions (Figure 1, blue line) showed that the rhodium atoms have reached a relatively equilibrated state in the silicon crystal lattice. The main diffraction peak was observed at  $2\theta = 28.45^\circ$ , and was identified as belonging to the (111)<sub>Si</sub> crystallographic orientation. The intensity of this peak was 860220 imp/s. The main The high intensity of the (111)<sub>Si</sub> reflection indicates that the overall order of the silicon crystal lattice is preserved. Despite the diffusion of the rhodium atoms, the main diamond structure of silicon has not been disturbed. The interlinear distance for this reflection was determined to be  $d = 3.136$  Å. The angular distribution of the peaks indicates that there is no significant change in the lattice constant, showing that the slow cooling process has resulted in a state close to thermodynamic equilibrium [19].

At the same time, an additional diffraction peak was observed in the X-ray diffraction pattern at  $2\theta = 32.2^\circ$ . This peak belongs to the SiRh<sub>3</sub> compound and corresponds to the (110) crystallographic direction. The SiRh<sub>3</sub> phase was found to possess tetragonal symmetry, with an interlinear spacing  $d = 2.778$  Å. This phase indicates that the rhodium atoms have chemically bonded with silicon. The SiRh<sub>3</sub> phase, formed under slow cooling conditions, can be considered to be primarily located at the sub-granular boundaries and in the near-surface layers. This is explained by the fact that the rhodium atoms lose their mobility after diffusion and settle into energetically favorable centres [20].

To assess the level of micro-stresses formed in n-Si<P,Rh> samples prepared under slow cooling conditions, the intensity ratio of the (222)<sub>Si</sub> and (111)<sub>Si</sub> reflections was calculated (see Fig. 2c, blue line). In the slow cooling regime, this ratio was  $I(222)/I(111) \approx 5.9 \cdot 10^{-4}$ . This value is small compared to the control samples, indicating that internal stresses in the crystal lattice have been partially relieved under the influence of the rhodium atoms. In the n-Si<P,Rh> samples prepared under rapid cooling conditions, the X-ray diffraction pattern differed significantly from that of the slow-cooling regime (Figure 1, brown line). The main (111)<sub>Si</sub> reflection was observed at  $2\theta = 28.42^\circ$ , and its intensity was noted to have decreased to 623 530 imp/s. The decrease in intensity is explained by the retention of a high degree of defects and micro-strains in the crystal lattice as a result of rapid cooling [21]. Under such conditions, the atoms do not have time to reach thermodynamic equilibrium and the existing structure remains in a ‘frozen’ state. X-ray diffraction patterns of n-Si<P,Rh> samples prepared under rapid cooling conditions show an additional peak at  $2\theta = 71.4^\circ$ . This peak corresponds to the RhO<sub>2</sub> oxide phase, which is represented by the (301) crystallographic orientation. It was determined that the RhO<sub>2</sub> phase has a tetragonal structure, with a crystallite size of approximately 8.5 nm and an interlinear distance of  $d = 1.325 \text{ \AA}$ . The formation of the RhO<sub>2</sub> phase indicates that the rhodium atoms actively reacted with oxygen under rapid cooling conditions [22]. This phenomenon clearly demonstrates the tendency of oxygen atoms to combine with rhodium, overcoming the background impurities present in silicon [23]. In n-Si<P,Rh> samples, the level of micro-stresses generated by rapid cooling increased significantly under the rapid cooling regime,  $I(222)/I(111) \approx 1.0 \cdot 10^{-3}$  (see the brown line in Fig. 2c). This value is considerably larger than that for the slow cooling regime, indicating that the rapid cooling process retains a high degree of internal strains in the crystal lattice [24].

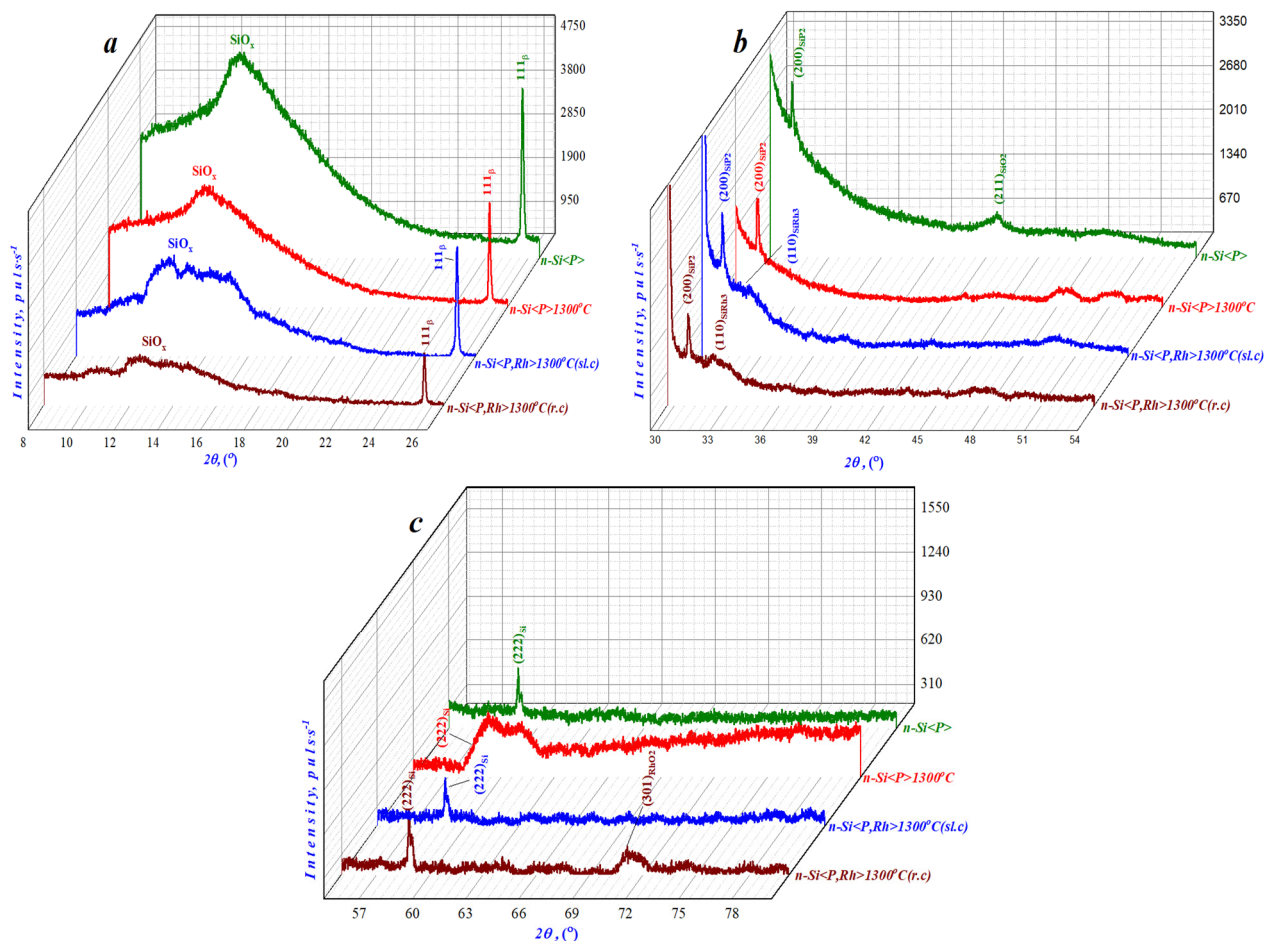


**Figure 2.** Enlarged XRD regions illustrating secondary phase formation and microstructural evolution in n-Si<P> and Rh-doped n-Si<P,Rh> single crystals: (a) low-angle region, (b) intermediate region, and (c) high-angle region.

### CONCLUSIONS

In the control samples, due to the redistribution of oxygen atoms in phosphorus and vanadium impurities as a result of high-temperature treatment, SiP<sub>2</sub> (polycrystallite size  $D \approx 88.4 \text{ nm}$ ) and secondary phases such as SiO<sub>2</sub> ( $D \approx 25 \text{ nm}$ ) were identified.

Heating at 1300°C for 5 hours leads to an increase in the silicon lattice constant to  $a \approx 5.4104 \text{ \AA}$  and a decrease in the diffraction reflection intensity, which was found to lead to an increase in microdeformations and scattering centers.

It was found that at the slow cooling (sc) rate, at the sub-granular partition boundaries, rhodium atoms chemically combine with silicon to form the tetrahedral SiRh<sub>3</sub> phase.

In rhodium-doped and slow-cooled samples, the degree of micro-stresses ( $I(222)/I(111) \approx 5.9 \cdot 10^{-4}$ ) is reduced compared to the control sample, indicating that the rhodium atoms possess the property of relieving internal lattice stresses.

It was found that during rapid cooling (rc), the rhodium atoms actively interact with the ambient oxygen to form the  $\text{RhO}_2$  oxide phase (crystallite size  $\approx 8.5$  nm), indicating the strong gettering property of rhodium.

During the rapid cooling process, the atoms do not have time to reach equilibrium, resulting in a high concentration of “frozen” defects in the crystal lattice and the retention of maximum micro-stresses ( $1.0 \cdot 10^{-3}$ )

#### Funding

The present research work was financed under the project FZ-292154210 granted by the Ministry of Innovative Development of the Republic of Uzbekistan

#### ORCID

©A.Y. Boboev, <https://orcid.org/0000-0002-3963-708X>; ©B.M. Ergashev, <https://orcid.org/0009-0007-9392-6548>;

©N.Y. Yunusaliyev, <https://orcid.org/0000-0003-3766-5420>; ©Z.M. Ibrokhimov, <https://orcid.org/0009-0003-6931-661X>;

©Sh.A. Makhmudov, <https://orcid.org/0009-0003-6539-9278>; ©A.K. Rafikov, <https://orcid.org/0000-0001-9199-2428>;

#### REFERENCES

- [1] J. Li, J. Wang, Z. Zhong, Z. Li, Y. Wen, L. Wang, and L. Liu, “Pathway and control of oxygen transport in the melt during single crystal silicon growth by continuous-feeding Czochralski method,” *Journal of Crystal Growth*, **662**, 128183 (2025). <https://doi.org/10.1016/j.jcrysgro.2025.128183>
- [2] W. Zhao, J. Li, and L. Liu, “Control of oxygen impurities in a continuous-feeding Czochralski-silicon crystal growth by the double-crucible method,” *Crystals*, **11**, 264 (2021). <https://doi.org/10.3390/cryst11030264>
- [3] R. Newman, “Oxygen diffusion and precipitation in Czochralski silicon,” *Journal of Physics: Condensed Matter*, **12**, R335 (2000). <https://doi.org/10.1088/0953-8984/12/25/201>
- [4] P. Dong, X. Liang, and D. Tian, “On the mechanism of carrier scattering at oxide precipitates in Czochralski silicon,” *Journal of Materials Science: Materials in Electronics*, **4**, (2015). <https://doi.org/10.1007/s10854-015-2728-6>
- [5] Y. Boboev, K. A. Makhmudov, and Z. M. Ibrokhimov, “Long-term relaxation processes of electrical conductivity in compensated Si<B,S> and Si<B,Rh> monocrystals,” *East European Journal of Physics*, (2), 436–440 (2025). <https://doi.org/10.26565/2312-4334-2025-2-54>
- [6] Sh. A. Makhmudov, A.A. Sulaymonov, and A.K. Rafikov, “Study of the concentration of Si impurities and their electrical state,” *Nauchnyi Zhurnal Fizika*, (1), 16 (2023). (in Russian, Kyrgyzstan)
- [7] J. Golubović, M. Varničić, and S. Štrbac, “Study of oxygen reduction reaction on polycrystalline rhodium in acidic and alkaline media,” *Catalysts*, **14**, 327 (2024). <https://doi.org/10.3390/catal14050327>
- [8] M. Trzcinski, G. Balcerowska-Czerniak, and A. Bukaluk, “XPS studies of the initial oxidation of polycrystalline Rh surface,” *Catalysts*, **10**, 617 (2020). <https://doi.org/10.3390/catal10060617>
- [9] Y. Boboev, B. M. Ergashev, N. Y. Yunusaliyev, and J. S. Madaminjonov, “Electrophysical nature of defects in silicon caused by implanted platinum atoms,” *East European Journal of Physics*, (2), 431–435 (2025). <https://doi.org/10.26565/2312-4334-2025-2-53>
- [10] Y. Boboev, S. K. Yulchiev, Z. M. Ibrokhimov, and N. Y. Yunusaliyev, “The impact of various lighting conditions on the photosensitive properties of Si<B,S> and Si<B,Rh> structures,” *East European Journal of Physics*, (4), 620–626 (2025). <https://doi.org/10.26565/2312-4334-2025-4-65>
- [11] X. Zhang and S. Wang, “Structure and growth of single crystal SiP<sub>2</sub> using flux method,” *Solid State Sciences*, **37**, 1–5 (2014). <https://doi.org/10.1016/j.solidstatesciences.2014.08.009>
- [12] A.Y. Boboev, B.M. Ergashev, N.Y. Yunusaliyev, and M.M. Xotamov, “Study of the formation of low-dimensional defect states in single-crystal silicon with the participation of oxygen,” *East European Journal of Physics* (2), 299–306 (2025). <https://doi.org/10.26565/2312-4334-2025-2-36>
- [13] K. Kayed and D. Kurd, “The effect of annealing temperature on the structural and optical properties of Si/SiO<sub>2</sub> composites synthesized by thermal oxidation of silicon wafers,” preprint, (2021). <https://doi.org/10.21203/rs.3.rs-246154/v2>
- [14] I.I. Gorbachev, E.I. Korzunova, V.V. Popov, D.M. Khabibulin, and N.V. Urtsev, “Simulation of austenite grain growth in low-alloyed steels upon austenitization,” *Physics of Metals and Metallography*, **124**(3), 303–309 (2023). <https://doi.org/10.31857/S0015323022601738>
- [15] K.S. Daliev, Sh.B. Utamuradova, J.J. Khamdamov, M.B. Bekmuratov, O.N. Yusupov, Sh.B. Norkulov, and Kh.J. Matchonov, “Defect formation in MIS structures based on silicon with an impurity of ytterbium,” *East European Journal of Physics*, (4), 301–304 (2024). <https://doi.org/10.26565/2312-4334-2024-4-33>
- [16] Geiskopf, M. Stoffel, and X. Devaux, “Formation of SiP<sub>2</sub> nanocrystals embedded in SiO<sub>2</sub> from phosphorus-rich SiO<sub>1.5</sub> thin films,” *The Journal of Physical Chemistry C*, **124**(14), 7973–7978 (2020). <https://doi.org/10.1021/acs.jpcc.9b11416>
- [17] J. Safarian, and M. Tangstad, “Phase diagram study of the Si–P system in Si-rich region,” *Journal of Materials Research*, **26**(12), 1494–1503 (2011). <https://doi.org/10.1557/jmr.2011.130>
- [18] L. Marot, R. Schoch, R. Steiner, V. Thommen, D. Mathys, and E. Meyer, “Rhodium and silicon system: II. Rhodium silicide formation,” *Nanotechnology*, **21**, 365707 (2010). <https://doi.org/10.1088/0957-4484/21/36/365707>
- [19] L. Schellenberg, J. L. Jorda, and J. Muller, “The rhodium-silicon phase diagram,” *Journal of the Less Common Metals*, **109**(2), 261–274 (1985). [https://doi.org/10.1016/0022-5088\(85\)90058-X](https://doi.org/10.1016/0022-5088(85)90058-X)
- [20] K. Matsukawa, K. Shirai, and H. Yamaguchi, “Diffusion of transition-metal impurities in silicon,” *Physica B: Condensed Matter*, **401–402**, 151–154 (2007). <https://doi.org/10.1016/j.physb.2007.08.134>
- [21] D. Garagnani, P. De Padova, C. Ottaviani, C. Quaresima, A. Generosi, B. Paci, B. Olivieri, *et al.*, “Evidence of sp<sup>2</sup>-like hybridization of silicon valence orbitals in thin and thick Si grown on  $\alpha$ -phase Si(111) $\sqrt{3} \times \sqrt{3} R30^\circ$ -Bi,” *Materials*, **15**(5), 1730 (2022). <https://doi.org/10.3390/ma15051730>

- [22] M. Trzcinski, G. Balcerowska-Czerniak, and A. Bukaluk, "XPS studies of the initial oxidation of polycrystalline Rh surface," *Catalysts*, **10**, 617 (2020). <https://doi.org/10.3390/catal10060617>
- [23] M.E. Turano, E.A. Jamka, M.Z. Gillum, and K.D. Gibson, "Emergence of subsurface oxygen on Rh(111)," *The Journal of Physical Chemistry Letters*, **12**(25), 5844–5849 (2021). <https://doi.org/10.1021/acs.jpcclett.1c01820>
- [24] Z.N. Weinrich, X. Li, S. Sharma, V. Craciun, M. Ahmed, E.A.C. Sanchez, S. Moffatt, and K.S. Jones, "Dopant-defect interactions in highly doped epitaxial Si:P thin films," *Thin Solid Films*, **685**, (2019). <https://doi.org/10.1016/j.tsf.2019.05.059>

#### СТРУКТУРНО-ФАЗОВІ СТАНИ МОНОКРИСТАЛІВ КРЕМНІЮ, ЛЕГОВАНИХ РОДІЄМ

Акрамжон Й. Бобоєв<sup>1</sup>, Шерзод А. Махмудов<sup>2</sup>, Аваз К. Рафіков<sup>2</sup>, Зійоджон М. Іброхімов<sup>3</sup>, Рахмат М. Мансуров<sup>4</sup>,  
Нурігдін Ю. Юнусалієв<sup>1</sup>, Білоліддін М. Ергашев<sup>5</sup>

<sup>1</sup>Андижанський державний університет імені З.М. Бабура, Андижан, Узбекистан

<sup>2</sup>Інститут ядерної фізики Академії наук Республіки Узбекистан

<sup>3</sup>Андижанський державний технічний інститут, Андижан, Узбекистан

<sup>4</sup>Академічний ліцей № 1 МВС Республіки Узбекистан

<sup>5</sup>Андижанський державний педагогічний інститут, Андижан, Узбекистан

У цій роботі досліджено структурний та фазовий стан монокристалів кремнію (Si), легованих атомами родію (Rh). Для дослідження було обрано зразки кремнію n-типу, леговані родієм, вирощені методом Чокральського. Атоми родію вводили шляхом термічної дифузії при 1300°C, а зразки охолоджували як у режимах повільного, так і швидкого охолодження. Отримані дані оцінювали за допомогою рентгеноструктурного аналізу (XRD). У контрольних зразках термічна обробка призвела до утворення вторинних фаз, таких як SiP<sub>2</sub> та SiO<sub>2</sub>, які, як було показано, пов'язані з фоновими домішками, зокрема атомами кисню. У зразку, легваному родієм та повільно охолоджену, утворилася фаза SiRh<sub>3</sub>, а кристалічна решітка залишалася відносно стабільною. Це вказує на те, що атоми родію мають здатність зменшувати внутрішні напруження та релаксувати решітку. У режимі швидкого охолодження з'явилася фаза оксиду RhO<sub>2</sub>, а також спостерігалася збільшення мікронапружень та кристалічних дефектів. Результати показують, що легування родієм є ефективним методом контролю структури, фазового складу та електричних властивостей монокристалів кремнію. Це дослідження має важливе значення для напівпровідникових матеріалів, мікроелектроніки та сонячних елементів.

**Ключові слова:** кремній; родій; фосфор; дифузія; домішка; кисень; вторинні фази; рентгенівська дифракція; дефекти; мікродеформація